Composites Part B 215 (2021) 108782

Contents lists available at ScienceDirect

Composites Part B

journal homepage: www.elsevier.com/locate/compositesb

Vitrimer chemistry enables epoxy nanocomposites with mechanical robustness and integrated conductive segregated structure for high performance electromagnetic interference shielding

Huagao Fang [a,b,*], Wujin Ye [a], Kangjie Yang [a], Kai Song [a], Haibing Wei [a,b], Yunsheng Ding [a,b,**]

[a] Department of Polymer Science and Engineering, School of Chemistry and Chemical Engineering, Hefei University of Technology, Hefei, Anhui, 230009, China
[b] Anhui Province Key Laboratory of Advanced Functional Materials and Devices, Hefei, Anhui, 230009, China

ARTICLE INFO

Keywords:
Epoxy vitrimer
Segregated nanocomposite
Interfacial welding
Mechanical robustness

ABSTRACT

Constructing segregated pathways in the conductive polymer composites (CPCs) is efficient to achieve satisfactory electrical conductivity and electromagnetic interference shielding effectiveness (EMI SE) with low content of nanofillers. Conventionally, most of segregated CPCs were based on thermoplastics and precisely controlled processing conditions were essential to achieve structural integrity and mechanical robustness. Herein, by taking the advantage of the associative dynamic bonding rearrangement in the epoxy vitrimer, we fabricated segregated MWCNTs/epoxy composites in a wide range of compression temperature and pressure. The segregated CPCs show a low conductive percolation threshold at 0.066 wt% and an EMI SE of 22 dB when only 2 wt% of MWCNTs were loaded. More promisingly, the mechanical robustness was achieved by the volatile ethylene glycol (EG) involved decomposition and repolymerization of β-hydroxyl ester at the interface even when numerous MWCNTs were in between. The segregated structure and macroscopic properties can be reserved after reprocessing and the nanofillers can be recovered with excessive EG at elevated temperature.

1. Introduction

The rapid development of electronic products in recent days has accompanied with the widespread concern of electromagnetic radiation pollution. Electromagnetic interference (EMI) generated by the increasing number of electronics not only leads to malfunctioning of adjacent devices but also seriously threatens the health of human beings and other animals [1]. Using electromagnetic interference shielding materials to attenuate EM wave has proven to effectively reduce the hazardous impact. The development of novel materials with high EMI shielding effectiveness (EMI SE) has become a highly desired requirement nowadays [2–5].

In comparison with metal materials, conductive polymer composites (CPCs) have received increasingly attention in the realm of EMI shielding due to their merits of lightweight, low cost, good processability, and corrosion resistance [6–9]. In a CPC, percolation threshold (ϕ_c) is defined as the critical content of conductive fillers, above which the composite transformed from an insulator to a conductor, often indicating the formation of a conductive network [10–15]. The ultralow percolation threshold is the goal to pursuit in many cases to reduce the consumption of expensive fillers, while the conventional CPCs often show high percolation threshold, which not only causes processing difficulties but also results in poor economic benefits [5,16]. Several researches have shown that constructing a segregated conductive network in CPCs is an effective way to achieve high EMI SE with low incorporation of conductive filler [17–20]. Through ingeniously designing the ingredients and precisely controlling the processing parameters, the conductive fillers can be selectively and directionally distributed in the matrix and formed an integrated conductive pathway, thus the amount of conductive filler necessary to form conductive pathway is much less than that in the randomly dispersed composites.

Compression molding of polymer particles wrapped by fillers is a commonly utilized method to fabricate composites with segregated structures. Thermoplastics with high viscosity and thermosets with loose

* Corresponding author. Department of Polymer Science and Engineering, School of Chemistry and Chemical Engineering, Hefei University of Technology, Hefei, Anhui, 230009, China.
** Corresponding author. Department of Polymer Science and Engineering, School of Chemistry and Chemical Engineering, Hefei University of Technology, Hefei, Anhui, 230009, China.
E-mail addresses: fanghg@hfut.edu.cn (H. Fang), dingys@hfut.edu.cn (Y. Ding).

https://doi.org/10.1016/j.compositesb.2021.108782
Received 22 January 2021; Received in revised form 28 February 2021; Accepted 8 March 2021
Available online 12 March 2021

crosslinking are the priority as the matrix to achieve the integrity of a segregated network. For example, ultrahigh molecular polyethylene (UHMWPE) was reported by several individual groups to be a suitable matrix to obtain well-segregated structure, which can prevent the migration of filler into the interior matrix during hot-pressing [21]. For some semi-crystalline polymers with low melt viscosity (e.g. polypropylene (PP) and polylactide (PLA)), special attention on the molding temperature below their melting temperature (T_m) should be paid to make the polymer matrix at solid state because once the molding temperature exceeds the T_m, the melt viscosity would dramatically decrease, which is unfavorable to maintain the segregated structure [22,23]. Another concern on segregated CPCs is their inferior mechanical performance, showing unsatisfactory strength and brittle nature. The conductive fillers located on the interface between particles would hinder the molecular diffusion across the boundary, resulting in inferior interfacial adhesion. Therefore, several efforts were deliberately made to circumvent this dilemma. Yan and coworkers successfully enhanced the compressive strength (108 MPa) of polystyrene insulation composites with 1.95 vol% rGO loading by increasing the compression pressure to as high as 350 MPa [24]. Wang and coworkers controlled the curing sequence of polydimethylsiloxane (PDMS) segregated phase and conductive phase, and used covalent bonds to strengthen the interface force, thereby improving the mechanical properties of the material [25]. Although much progress has been accomplished so far, there is still a challenge to prepare segregated CPCs with sufficient mechanical robustness.

Vitrimers, as a new group of crosslinked polymers, can rearrange their network topology through thermally activated bond exchange reaction (BER), including disulfide exchange [26], olefin metathesis [27], boronic ester exchange [28], β-hydroxyl esters [29] and so on. Because of the associative mechanism of dynamic covalent β-hydroxyl ester in epoxy vitrimers (EV), the cross-linking density remain unchanged during network rearranging, showing the viscosity decreases gradually with increasing temperature and is consistent with an Arrhenius-type dependence. In addition to the typical glass transition temperature (T_g) of polymers, there is also a topological transition temperature (T_v) for vitrimers, which can be determined from stress relaxation and dilatometry measurements. Our previous work revealed that EV experiences a critical rheological transition state at T_v and then proposed a facile method to measure it [30]. Since the first report in 2011, several other vitrimeric and vitrimer-like materials were developed and viewed as the most striking accomplishment in the area of glassy polymers in the last decade [31,32]. Surface welding and reprocessing of epoxy vitrimer were accelerated with the assistance of ethylene glycol (EG) as an active solvent [33,34]. Several nanocomposites with excellent performance based on epoxy vitrimer were developed, showing great potentials in the application as functional materials [35–37].

Herein, we report a novel and facile method to fabricate the EMI shielding composites with a segregated structure using an epoxy vitrimer as the matrix. Taking advantage of its vitrimeric characteristic in rheology and dynamic chemistry, compression molding in a wide range of temperatures and pressure can achieve integrated segregation and remarkable improvement in mechanical properties. The effects of incorporating MWCNTs content on the electrical conductivity and EMI shielding performance were investigated in this work. Reprocessing and recycling of the composites were also discussed.

2. Experimental

2.1. Materials

Diglycidyl ether of bisphenol A (DGEBA, DER 332) and Zinc acetate dihydrate were purchased from Sigma-Aldrich (Shanghai, China). Pripol 1040 was kindly provided by Croda (Netherlands), which is a mixture of polymerized fatty acid containing about 82 wt % trimers and 18 wt % dimers according to the manufacturer. Multiwall carbon nanotubes (MWCNTs, XFM13) with the length of 10–30 μm and the diameter of 10–20 nm were supplied by Jiangsu XFNANO Materials Tech Co., Ltd., China. Ethylene glycol (EG) with a purity of 99% was obtained from Macklin Inc (Shanghai, China).

2.2. Sample preparation

The brief description on the preparation of the epoxy vitrimer (EV) is presented as follows: Zinc acetate dihydrate (10 mol% to the epoxy groups) was mixed with Pripol 1040 and gradually heated from 100 to 180 °C with vigorously stirring and gradually increasing the vacuum in a three-neck flask equipped with a mechanical stir. When the temperature reached 180 °C, it was maintained for 2 h until no bubbles were generated. After that, the temperature was lowered and maintained at 75 °C, and then a certain amount of DGEBA was added and mechanically stirred for 30 min. The stoichiometric ratio of the carboxyl to epoxy groups in the mixture was fixed at 1:1. The mixture was then introduced into a tetrafluoroethylene mold and cured at 130 °C for 6 h in vacuum. The cured sample was pulverized and the particles in diameter of 40–80 μm were selected by a sieving method. The segregated EV/MWCNTs composites were fabricated according to the following procedure: MWCNTs were first added to 100-fold of a mixture of EG/ethanol (1/50 in volume ratio) and sonicated to a stable dispersion using an ultrasonic cell crusher. Then, the preweighted EV particles were slowly added into the MWCNTs dispersion and after stirring for 30 min, the suspension was filtered with a Buchner funnel under reduced pressure. The EV particles wrapped with MWCNTs were dried at room temperature and hot-pressed to obtain the resultant composites under pre-defined temperature and pressure. The weight fraction of MWCNTs in the segregated EV composites is 0.1, 0.25, 1, 2, and 4 wt%, respectively. The segregated sample is coded as EV/MWCNTs-x, in which x indicates the content of MWCNTs. The EV composites with randomly distributed MWCNTs (denoted as uni-EV/MWCNTs-x) were also fabricated for comparison.

2.3. Characterization

The dispersion of MWCNTs on the EV particle surface was investigated by a field emission scanning electron microscope (SEM, Zeiss, Germany). The morphology of EV particles and segregated structures of MWCNTs in the matrix were observed using an optical microscope (OM, Olympus, Japan) and the size distribution was determined by analyzing the several images with ImageJ software. The segregated EV composites were cut into 20 μm-thick films using a microtome before observation. The mechanical properties were evaluated on a CMT4101 electromechanical universal testing machine (SANS, China) and the crosshead speed was 10 mm/min. The thermal properties were measured on a Q2000 differential scanning calorimetry (DSC, TA Instruments, USA) with the heating and cooling rate at 10 °C/min to investigate the glass transition temperature. The rheological properties were measured by using a DHR-1 rotary rheometer (TA Instruments, USA) under the nitrogen atmosphere in parallel plates with diameters of 8 mm. The electrical conductivity was investigated by a high resistance test instrument (Shanghai Anbiao Electronics Co., Ltd., China) or a four-point probe (RTS-8, Guangzhou Four-Point Probe Technology Co., Ltd., China). At least three specimens were tested and the average data was given. A vector network analyzer (N5247A, Agilent Technologies, USA) was used to measure the EMI SE of the segregated sample in the X-band at room temperature via the coaxial method. The samples were compressed into φ12 mm circular sheets with a thickness of 2 mm for the test. The 2-port thru-reflect-line (TRL) calibration was performed before measurement to ensure the data reliability. Infrared spectra of different parts in the segregated structure were investigated on a Nicolet iS50 Fourier transform infrared spectroscopy with an attenuated total reflection assemble (ATR-FTIR, Thermo Scientific, USA).

3. Results and discussion

3.1. Fabrication of the EV/MWCNTs composites with segregated structure

As shown in Fig. 1a, the EV matrix was prepared by the reaction of epoxy groups on DGEBA with the carboxylic acid on the multifunctional polymerized fatty acid derivatives following the recipe and method in the literature [38]. The EV can flow by rearranging their network topology above T_v of around 75 °C through thermally triggered transesterification reactions under Lewis acid catalysis. For fabricating the segregated composites, the fully crosslinked EV sheets were first pulverized and sieved to obtain small-sized particles. As shown in Fig. 1b, the EV particles with relatively wide size distribution were successfully obtained after pulverization and sieving, in which the majority of particle size distribution was in the range of 40–80 μm. In this process of liquid-phase adsorption deposition (Fig. 1c), the MWCNTs were first dispersed in ethanol/EG mixture with the aid of ultra-sonication and then added the fresh pulverized EV particles. As compared in Fig. S1 in the supplementary materials, MWCNTs can be suspended in ethanol after cease of sonication for 3 h. However, when EV particles were added and stirred, due to the electrostatic adsorption in between, the MWCNTs quickly adhered to the surface of EV particles and precipitated within 30s. A similar method was reported in preparing dynamic crosslinked flexible polyurethane composite [39]. SEM observation shows that the EV particles before MWCNTs wrapping had an irregular shape and smooth surface. The surface became rough after wrapping and was observed to be uniformly covered with numerous MWCNTs, which could benefit the formation of a segregated structure.

3.2. Interfacial welding by volatile EG involved bond exchange reaction

In the conventional compression molding, it is usually necessary to precisely control the processing parameters to gain a segregated structure, which is inconvenient in practical applications. For example, the narrow temperature window or high compression pressure is usually preferred to gain a well-segregated morphology. Meanwhile, it is not always easy to implement mechanical robustness. The bonding of polymer particles originated from the physical interaction between macromolecular chains that diffused across the phase boundary and their entanglements. However, the conductive fillers which located on the interface would hinder the diffusion, resulting in inferior interfacial adhesion and poor mechanical strength in some cases.

In the current study, the fully crosslinked epoxy vitrimer was used as the matrix. Due to the associative BER mechanism, the cross-linking density remains unchanged in the topological rearrangement and the viscosity only experiences marginal change within a broad temperature range, in line with the so-called Arrhenius-type dependence on temperature. As depicted in Fig. 2a, the small-amplitude oscillation shear (SAOS) rheology measurement reveals the elastomeric characteristics of the sample, showing the storage modulus G′ larger than the loss modulus G″ in the whole measuring frequencies. The marginal changes in modulus and viscosity (see Fig. S2) indicate its Arrhenius-type dependence on temperature, maintaining its elastic network state within the range of test temperatures, which provide a promising opportunity to fabricate segregated polymer composites in a broader compressing temperature and pressure range. As a proof of concept, we tentatively hot pressed the wrapped EV particles at different temperatures (150 °C and 180 °C) under different pressure loads (4 MPa and 10 MPa). It is seen in Fig. 2b that the complete conductive network pathways can be formed and the well-defined segregated structures remain unbroken under each processing condition, indicating the penetration of MWCNTs into the matrix is greatly retarded by the crosslinked structure. A careful comparison of the three optical micrographs in Fig. 2b reveals that the sample from higher temperature and pressure (180 °C and 10 MPa) showed denser MWCNTs domains than the previous two samples, indicating that the degree of interfacial bonding is improved by increasing of pressure and temperature.

The decomposition and repolymerization of transesterification

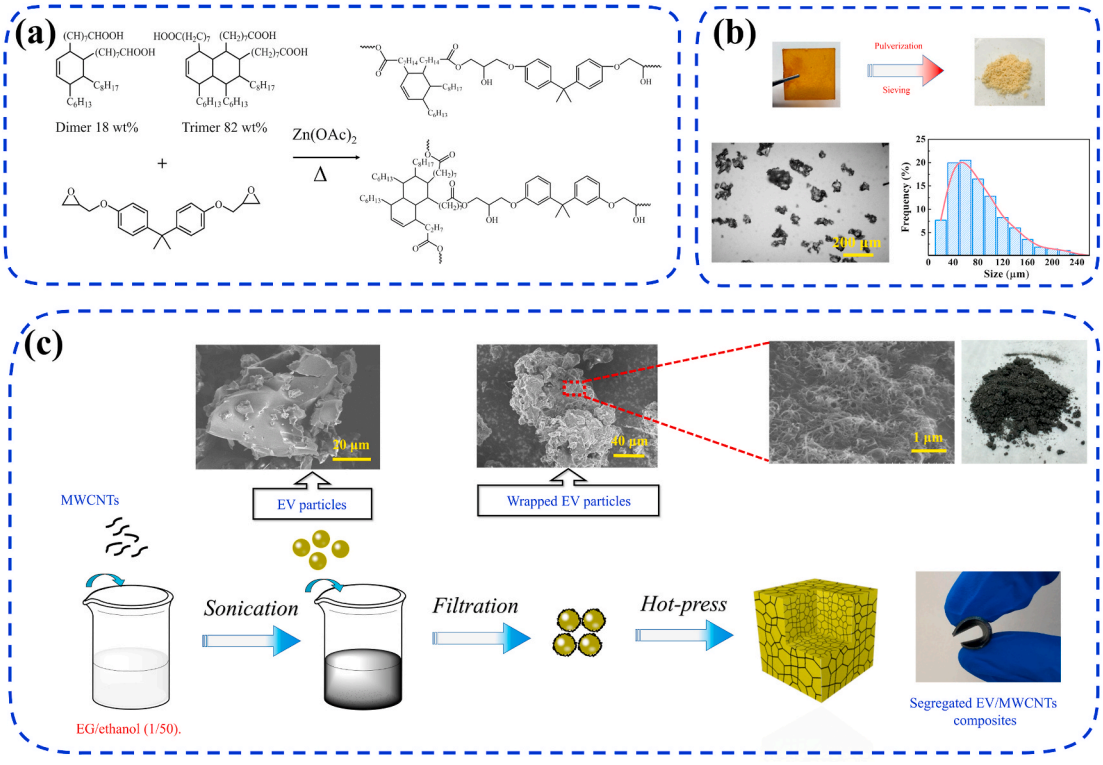

Fig. 1. (a) Synthesis of the EV by the reaction of epoxy groups with carboxylic groups from the fatty acid derivatives. (b) Particle size distribution histogram of EV particles obtained from pulverization and sieving. (c) Schematic illustration of the fabrication of the segregated EV/MWCNTs composites by compression molding.

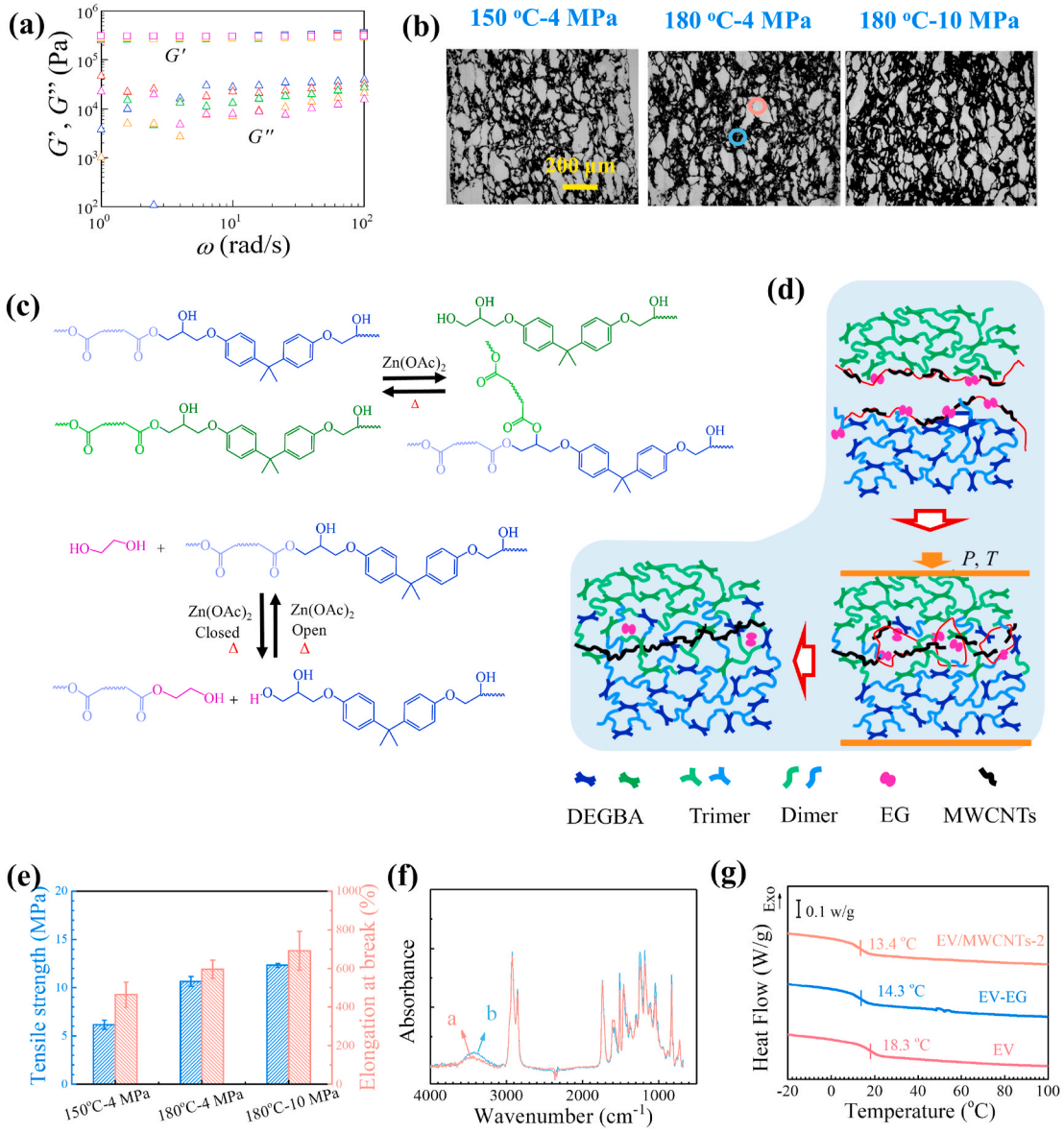

Fig. 2. (a) Rheological properties for EV at different temperatures. The temperatures are 100 (blue), 120 (red), 140 (green), 160 (magenta) and 180 °C (brown), respectively. (b) Optical microscopy images of the cross-section of the segregated EV composites with 2 wt% of MWCNTs from mold compression under different processing conditions. The scale bar in the left image represents 200 μm and is applied to other images. (c) The structural rearrangement through thermally triggered catalytic transesterification reaction and the decomposition and repolymerization of ester bond incorporated by EG molecules. (d) Schematic illustration of interfacial welding enabled by EG incorporated reaction under elevated temperature and pressure. (e) Mechanical properties of the segregated EV composites. (f) FTIR spectra of the different parts in the segregated structure. (g) DSC curves for neat EV, the welded EV with EG assistance, and the segregated EV/MWCNTs-2 composite. (For interpretation of the references to colour in this figure legend, the reader is referred to the Web version of this article.)

enabled by small-molecule additives were adopted to accelerate the transesterification reaction and improve the mechanical robustness for the segregated composite [33,40]. The structural rearrangement through thermally triggered catalytic transesterification reaction and the decomposition and repolymerization mechanism enabled by EG are shown in Fig. 2c, respectively. When heated above T_v, the transesterification of β-hydroxyl esters is activated to rearrange its network, in which the sufficient hydroxyl groups play a key role to spur its topological rearrangement [41]. When bifunctional EG molecules are added, the hydroxyl groups participate in the transesterification reactions with ester groups in the dynamic network, resulting in breaking the network into highly mobile short-chain components. These could facilitate the penetration of polymer chains across the boundary and build up the interfacial bonding over the obstacle of MWCNTs. When heated at a moderate temperature of 180 °C in an open atmosphere, the EG molecules tend to evaporate and the repolymerization becomes dominant, resulting in the recovery of network structure. Applying external pressure will accelerate the process by better contact and contribute to interfacial welding of wrapped EV particles even when some MWCNTs are located on the boundary (see Fig. 2d). For highlight the contribution of EG, we also performed a control experiments in which the wrapped EV particles without adding EG were hot-pressed under the same condition and found that the particles were poorly welded and some cracks still remained in the obtained specimen. (Fig. S3).

The uniaxial extension was further performed to testify the integrity and robustness of the segregated structure. As shown in Fig. 2e, the considerable mechanical robustness (6.2 MPa in strength and 460% in elongation at break) is achieved even for the sample obtained from the lowest processing temperature and pressure, indicating that interfacial

vitrimer chemistry has great potential to bond the segregated polymer composites. With increasing temperature and pressure, their mechanical properties can be further improved, which is ascribed to the formation of more chemical bonding to facilitate the effectiveness of the stress transfer in the matrix by overcoming the hindrance of the wrapped MWCNTs. The representative red and blue areas of the welded composite in Fig. 2b were measured using FTIR to explore possible chemical structure changes. The corresponding FTIR curves are shown in Fig. 2f. After normalizing the peak intensity of ester groups at 1725 cm^{-1}, the hydroxyl peak (3400 cm^{-1}) in the interfacial zone is significantly increased as compared with the matrix. This indicates that EG molecules participate in the reaction to weld the matrix and some of them might remain at the end of the residual short-chain components in the composite. It should be noted that due to its small content and locally distribution, it is difficult to determine the exact residual fraction of EG and our FTIR measurement can only qualitatively reveal its participation in the interfacial welding. DSC measurements in Fig. 2g further show the decrease of the glass transition temperature (T_g) after welding, reflecting that the plasticity of the composite material is improved by residual short-chain components.

In the subsequent work, Compression molding at 180 °C under 4 MPa for 15 min was adopted to prepare the segregated EV composites for further investigation on the effect of different content of MWCNTs incorporation.

3.3. Mechanical property and stress relaxation behavior

The representative stress–strain curves of the segregated EV/MWCNTs composites with various MWCNTs loadings are compared in Fig. 3a and the corresponding parameters are listed in Fig. 3b. Neat EV shows stiff elastomeric deformation under stretching, showing the high Young's modulus and moderate elongation at break. In the welded samples with MWCNTs, the mechanical properties experience an evolution of first increase and then decrease with increasing of MWCNTs. When the content of MWCNTs is 0.25 wt%, the elongation at break can reach to 761% with the tensile strength of 14.5 MPa and the tensile toughness of 44.4 MJ m^{-3}. The significantly enhanced mechanical properties can be ascribed to the rebuilding of covalent bonds by the transesterification in the interfacial zone. As discussed in the preceding section, the decomposition and repolymerization of dynamic network enabled by the volatile EG molecules provide "active glue" to adhere to the separated particles and facilitate the interfacial strength even when a considerable amount of MWCNTs are located in between. When the content of MWCNTs is increased to 2 wt%, the mechanical properties slightly decrease, but remain 90% of the tensile strength of its parent matrix. Remarkably different from the conventional polymer nanocomposites in which the uniformly dispersed nanofillers could retard the mobility of the neighboring molecular segments and thus improve the T_g value [42,43], the T_g of our composites decreases with the increase of MWCNTs (Fig. 3c). It is possible that more amount of EG molecules are entrapped on the surface with increasing of MWCNTs, leading to more content of small molecular component and the improved chain mobility.

The effect of MWCNTS on the dynamic vitrimeric properties of the segregated composites were investigated. Before stress relaxation measurement, the thermal stability was first checked and the results are shown in Fig. S4. The normalized relaxation modulus for the segregated EV composites were shown in Fig. 3d. As expected, the stress relax with time for all samples, reflecting the dynamic vitrimeric properties that

(b)

Sample code	Tensile strength (MPa)	Elongation at break (%)	Young's modulus (MPa)	Tensile toughness (MJm^{-3})
EV	12.0 ± 0.3	415 ± 51	22.7 ± 0.5	27.7 ± 4.2
EV/MWCNTs-0.25	14.5 ± 1.0	761 ± 106	10.0 ± 0.2	44.4 ± 4.9
EV/MWCNTs-1	12.7 ± 0.6	705 ± 25	7.3 ± 0.2	37.1 ± 1.7
EV/MWCNTs-2	10.8 ± 0.6	588 ± 53	4.1 ± 0.1	29.8 ± 1.4
EV/MWCNTs-4	5.2 ± 0.9	542 ± 112	5.7 ± 0.1	17.0 ± 1.9

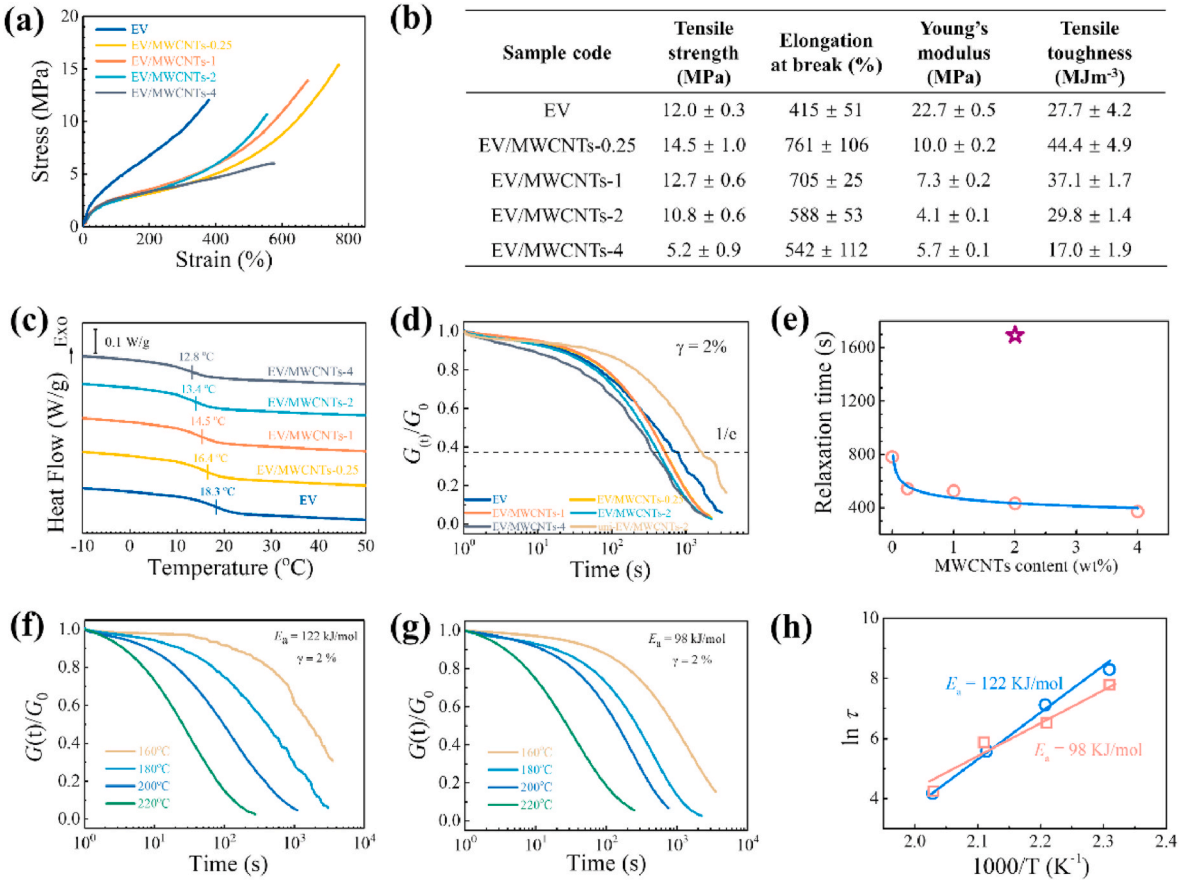

Fig. 3. (a) Representative strain-stress curves, (b) table of the mechanical parameters, (c) DSC curves, and (d) stress relaxation curves for the segregated EV/MWCNTs composites. (e) Change of the characteristic relaxation times as a function of MWCNTs content. Stress relaxation curves for (f) neat EV and (g) the segregated EV/MWCNTs-2 at different temperatures. (h) Arrhenius plot of the relaxation times for neat EV and the segregated EV/MWCNTs-2.

can flow at elevated temperatures. The sample with more MWCNTs can relax faster, suggesting that the less degree of crosslinking in the interfacial area can relax its inner stress easier, which is consistent with the DSC results. The characteristic relaxation times (τ, defined as the time at 1/e of the normalized relaxation stress) are collected and presented in Fig. 3e. The relaxation time for neat EV is 780s, but in striking contrast, the relaxation time for uni-EV/MWCNTs-2 is much longer (τ = 1694s), because the uniformly dispersed MWCNTs in the matrix slow down the BER and prolong the relaxation process. A similar increase has been reported in EV-silica nanocomposites [44] and dynamic boronic ester cross-linked epoxidized natural rubber/CNTs vitrimer composites [45]. With the increase of MWCNTs, the τ of the segregated composites is accelerated gradually from 532s for EV/MWCNTs-0.25 to 360s for EV/MWCNTs-4. The effect of temperature on stress relaxation behaviors of neat EV and the segregated EV/MWCNTs-2 are shown in Fig. 3f and g, respectively. It is obvious that the relaxation rate is accelerated with temperature and the relaxation times also show an Arrhenius-like temperature dependence $\tau_{(T)} = \tau_0 \exp(E_a/RT)$ (Fig. 3h), which further indicates the associative exchange mechanism. Accordingly, the transesterification activation energy E_a for EV/MWCNTs-2 is 98 kJ/mol, which is significantly lower than that of neat EV (122 kJ/mol). It is noted that the welded EV with EG assistance shows an E_a of 110 kJ/mol in Fig. S5. We can conclude that the acceleration of the stress relaxation process in the segregated EV/MWCNTs composites is ascribed to the reduced cross-linked networks by the residual EG molecules. In a more loosely cross-linked network, the chain mobility and the reactive group diffusion are less restricted, which consequently boost bond reshuffling and decrease the activation energy.

3.4. Electrical conductivity and EMI shielding performance

The presence of conductive MWCNTs with segregated distribution possesses substantial effects on their electrical conductivity and EMI shielding performance. The optical microscope (OM) images of the cross-section of the composites were depicted in Fig. 4a. The sample with 0.1 wt% MWCNTs already shows some connected nanotubes between neighboring EV particles to form conductive pathways. However, the segregated conductive pathways are not uniform. As the content of MWCNTs increases, the black layers become significantly thicker and denser, indicating an integrated conductive network was formed inside the segregated EV/MWCNTs composites.

The electrical conductivity, σ, is consistent with the above direct optical observation(Fig. 4b), showing soaring with the increase of MWCNTs. Neat EV is an insulator with σ in the order of 10^{-14} S/m. It experiences a sharp increase to 1.5 × 10^{-2} S/m when 0.25 wt% of MWCNTs is incorporated, which is a 12-decade improvement. Beyond this content, the gradual improvement of the electrical conductivity can be obtained, which reaches 2.0 and 6.8 S/m when 2 and 4 wt% of MWCNTs are loaded, respectively. According to the classical percolation theory [8,46] as described in the supplementary materials, an percolation threshold of 0.066 wt% (0.040 vol%) (Fig. 4c) was obtained from the optimized fitting, which is a low value compared with other reported epoxy/MWCNTs composites materials with segregated or uniformly dispersed structures [18,47–49], and a specific comparison of percolation threshold is showed in the Tab. S1. It is known that a three-dimensional network is obtained in CPCs when the critical exponent $t > 2$, otherwise a two-dimensional network structure is obtained when the value of $t < 2$ [50,51]. The ultralow percolation threshold and three-dimensional (t = 2.4) network indicate that compression molding

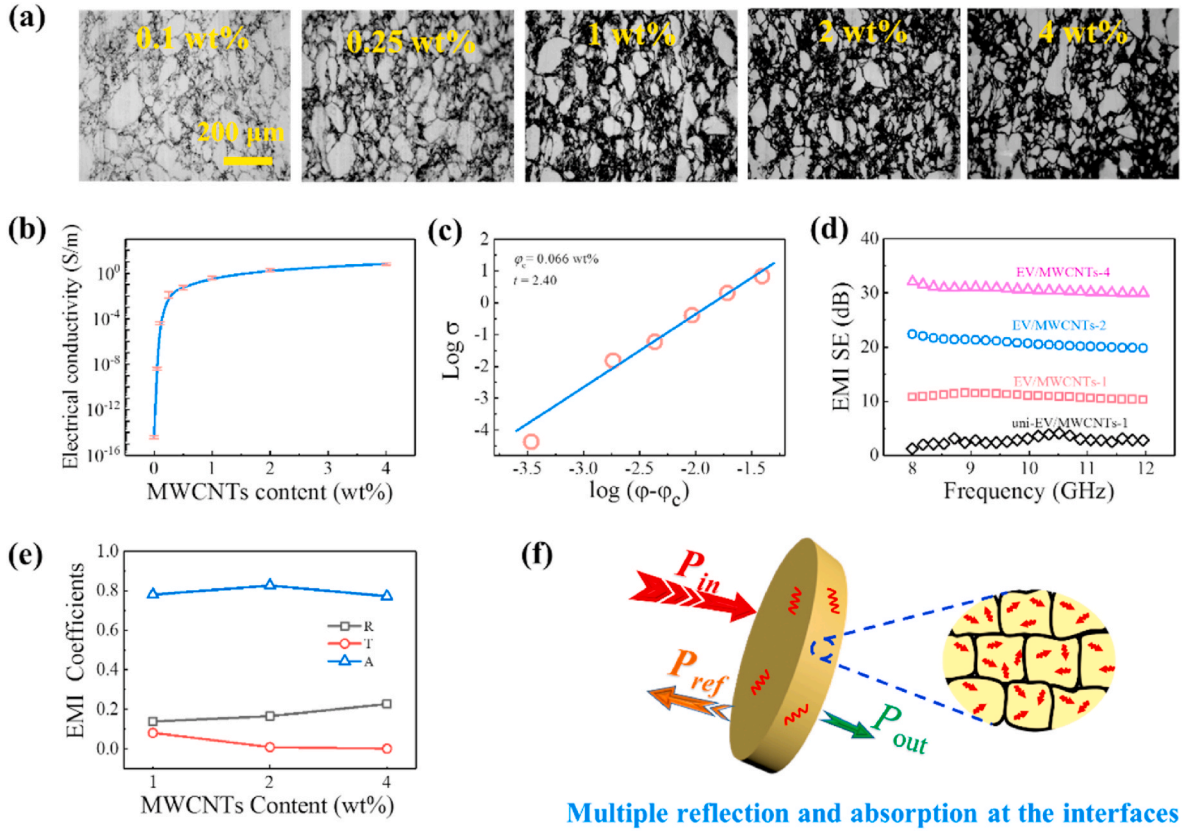

Fig. 4. (a) OM images of the segregated EV composites with different MWCNTs contents. (b) The electrical conductivity of the segregated EV composites as a function of MWCNTs content. (c) The fitting according to the percolation theory. (d) EMI SE as a function of frequency for the segregated EV/MWCNTs with different MWCNTs contents. (e) Comparison of the EMI coefficients of reflectivity (R), absorptivity (A), and transmissivity (T). (f) Schematic illustration of the EMI shielding mechanism for the segregated EV/MWCNTs composites.

MWCNTs wrapped vitrimer particles was proven to be an efficient and facile method to fabricate nanocomposites with integrated segregation of different components.

The EMI shielding performance is presented in Fig. 4d, showing that EMI SE increases with the MWCNTs content. The composites show an EMI SE of 22 dB when only 2 wt% of MWCNTs are loaded and increase to 31.5 dB with 4 wt% of MWCNTs. The significant improvement in EMI SE after incorporating small fraction of MWCNTs is attributed to the formation of segregated conductive networks. As compared the samples with 1 wt% loading, the segregated structure exhibits superior EMI shielding performance, in which the conductive pathway is easy to form. While in randomly dispersed composites, most of MWCNTs cannot connect to form pathways of electrons and the incident electromagnetic waves are not dissipated in large quantities. To understand the shielding mechanism, the corresponding power coefficients of reflectivity (R), absorptivity (A), and transmissivity (T), which were calculated from S parameters, are employed to evaluate the power balance of electromagnetic waves interacting with the segregated composites and the results are plotted as the function of MWCNTs content (Fig. 4e). The detailed calculation process is presented in the Supplementary Materials. It is clearly observed that the value of A is always higher than R, indicating that the absorption mechanism dominates EMI shielding regardless of MWCNTs content. As schematically shown in Fig. 4f, due to the segregated structure, where highly conductive skeleton (the segregated MWCNT network) provides multiple reflection, whereas the absorption takes place in the dielectric parts of the structure surrounded by conductive segregated network, which make the microwaves difficult to transmit before being absorbed. A similar shielding mechanism has been reported for many CPC foams or porous carbon monoliths, in which conductive cells are also commonly existed [52–54].

3.5. Reprocessing and recycling performance

The reprocessing of the composites and recycling of the epoxy matrix and MWCNTs was investigated using EV/MWCNTs-2 as an example. As demonstrated in the preceding section, our segregated EV composites could rearrange the network topology through the transesterification to completely relax stress at elevated temperatures. As shown in Fig. 5a, EV/MWCNTs-2 was manually grinded into particles and hot-pressed into a disc-shaped sample using the same condition (at 180 °C under 4 MPa for 15 min). It is obvious that the integrated disc was readily obtained after reprocessing for three times. Optical observation shows the segregated structure is somehow deteriorated with increasing of reprocessing iteration (Fig. 5b). The improved direct contact of the polymeric matrix after reprocessing can enhance its mechanical toughness, showing the comparable strength and remarkable increase of elongation at break in Fig. 5c. It should be noted that the declining of the integrated segregation results some negative effects on the electrical conductivity and EMI shielding performance (Fig. 5d and e), which could be avoided by additionally wrapping MWCNTs before compression in every reprocessing iteration.

The recycling of some expensive fillers is an important concern in the sustainable development of nanocomposites. The dissolution method was adopted to recover MWCNTs in this work. As shown in Fig. 5f, EV/MWCNTs-2 cannot be dissolved when immersed in trichlorobenzene for 7 days, verifying its covalently crosslinked structure. On the other hand,

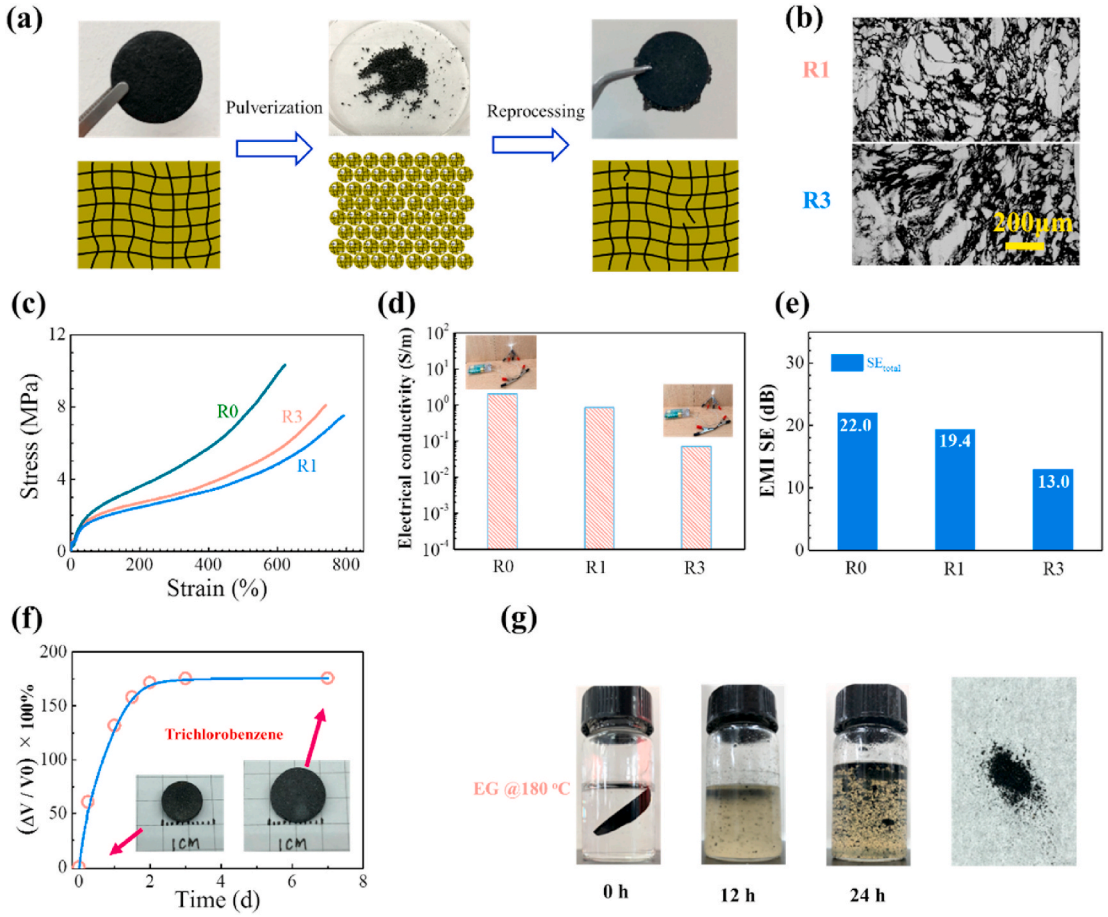

Fig. 5. (a) Schematic illusion of reprocessing of the segregated composites. (b) OM images, (c) stress-strain curves, (d) electrical conductivity, and (e) EMI SE of EV/MWCNTs-2 after reprocessing. (f) The swelling experiment in trichlorobenzene at room temperature. (g) Alcoholysis of EV/MWCNTs-2 at 180 °C and the recovery of MWCNTs.

the sample could react with sufficient EG, leading to the depolymerization of network. Fig. 5g shows successive dissociation of the composite was achieved by immersing in EG solution at 180 °C in 24 h. Most of the incorporated MWCNTs were then recovered by flushing with alcohol.

4. Conclusions

In this work, we introduced epoxy vitrimer as the matrix to fabricate high performance EMI shielding materials with segregated structure. The integrity of MWCNTs segregation is reserved under moderate and broad conditions in compression molding, ranging from 140 to 180 °C in temperature and from 4 to 10 MPa in pressure. Accordingly, the excellent electrical conductivity and EMI shielding performance are achieved with low MWCNTs loading. The segregated boundary at the presence of conductive fillers is reconnected by the repolymerization of β-hydroxyl ester after the removal of volatile ethylene glycol molecules, resulting in the significantly improved mechanical properties. The reprocessability of the segregated samples is achieved when the pulverized composite particles is re-pressed under the same conditions, maintaining the well segregated distribution of MWCNTs. Our work provides a novel and facile route to fabricate flexible CPCs with simultaneously high performance EMI SE and superior mechanical robustness, which could have potential applications in flexible electronics packaging. Their merits of reprocessaiblity and recyclability could also contribute to the sustainable development of EMI shielding materials.

CRediT authorship contribution statement

Huagao Fang: Investigation, Supervision, Writing- review & editing, Funding acquisition. **Wujin Ye:** Methodology, Writing - original draft. **Kangjie Yang:** Methodology. **Kai Song:** Investigation. **Haibing Wei:** Writing - review & editing. **Yunsheng Ding:** Supervision, Funding acquisition

Declaration of competing interest

The authors declare that they have no known competing financial interests or personal relationships that could have appeared to influence the work reported in this paper.

Acknowledgments

This work was financially supported by the National Natural Science Foundation of China (Grant Nos. 51503055 and 51673056) and the Fundamental Research Funds for the Central Universities (Grant No. PA2020GDKC0009).

Appendix A. Supplementary data

Supplementary data to this article can be found online at https://doi.org/10.1016/j.compositesb.2021.108782.

References

[1] Engels S, Schneider NL, Lefeldt N, Hein CM, Zapka M, Michalik A, Elbers D, Kittel A, Hore PJ, Mouritsen H. Anthropogenic electromagnetic noise disrupts magnetic compass orientation in a migratory bird. Nature 2014;509(7500):353–6.
[2] Chung DDL. Electromagnetic interference shielding effectiveness of carbon materials. Carbon 2001;39:279–85.
[3] Shahzad F, Alhabeb M, Hatter CB, Anasori B, Man Hong S, Koo CM, Gogotsi Y. Electromagnetic interference shielding with 2D transition metal carbides (MXenes). Science 2016;353(6304):1137–40.
[4] Wang L, Shi X, Zhang J, Zhang Y, Gu J. Lightweight and robust rGO/sugarcane derived hybrid carbon foams with outstanding EMI shielding performance. J Mater Sci Technol 2020;52:119–26.
[5] Zhang Y, Si H, Liu S, Jiang Z, Zhang J, Gong C. Facile synthesis of BN/Ni nanocomposites for effective regulation of microwave absorption performance. J. Alloy. Compd. 2021;850:156680.
[6] Jiang D, Murugadoss V, Wang Y, Lin J, Ding T, Wang Z, Shao Q, Wang C, Liu H, Lu N, Wei R, Subramania A, Guo Z. Electromagnetic interference shielding polymers and nanocomposites - a review. Polym Rev 2019;59(2):280–337.
[7] Abbasi H, Antunes M, Velasco JI. Recent advances in carbon-based polymer nanocomposites for electromagnetic interference shielding. Prog Mater Sci 2019;103:319–73.
[8] Fang H, Wang S, Ye W, Chen X, Wang X, Xu P, Li X, Ding Y. Simultaneous improvement of mechanical properties and electromagnetic interference shielding performance in eco-friendly polylactide composites via reactive blending and MWCNTs induced morphological optimization. Compos B Eng 2019;178:107452.
[9] Chen Z, Xu C, Ma C, Ren W, Cheng HM. Lightweight and flexible graphene foam composites for high-performance electromagnetic interference shielding. Adv Mater 2013;25(9):1296–300.
[10] Liu H, Gao J, Huang W, Dai K, Zheng G, Liu C, Shen C, Yan X, Guo J, Guo Z. Electrically conductive strain sensing polyurethane nanocomposites with synergistic carbon nanotubes and graphene bifillers. Nanoscale 2016;8(26):12977–89.
[11] Song P, Liu B, Liang C, Ruan K, Qiu H, Ma Z, Guo Y, Gu J. Lightweight, flexible cellulose-derived carbon aerogel@reduced graphene oxide/PDMS composites with outstanding EMI shielding performances and excellent thermally conductivities. Nano-Micro Lett 2021. https://doi.org/10.1007/s40820-021-00624-4.
[12] Li J, Ma P, Chow WS, To CK, Tang B, Kim JK. Correlations between percolation threshold, dispersion state, and aspect ratio of carbon nanotubes. Adv Funct Mater 2007;17(16):3207–15.
[13] Yu W, Zhang G, Liu Y, Xu L, Yan D, Huang H, Tang J, Xu J, Li Z. Selective electromagnetic interference shielding performance and superior mechanical strength of conductive polymer composites with oriented segregated conductive networks. Chem Eng J 2019;373:556–64.
[14] Zhang Y, Ruan K, Shi X, Qiu H, Pan Y, Yan Y, Gu J. Ti3C2Tx/rGO porous composite films with superior electromagnetic interference shielding performances. Carbon 2021;175:271–80.
[15] Song P, Liu B, Qiu H, Shi X, Cao D, Gu J. MXenes for polymer matrix electromagnetic interference shielding composites: a review. Compos Commun 2021;24:100653.
[16] Sang G, Dong J, He X, Jiang J, Li J, Xu P, Ding Y. Electromagnetic interference shielding performance of polyurethane composites: a comparative study of GNs-IL/Fe3O4 and MWCNTs-IL/Fe3O4 hybrid fillers. Compos B Eng 2019;164:467–75.
[17] Pang H, Xu L, Yan D, Li Z. Conductive polymer composites with segregated structures. Prog Polym Sci 2014;39(11):1908–33.
[18] Feng D, Xu D, Wang Q, Liu P. Highly stretchable electromagnetic interference (EMI) shielding segregated polyurethane/carbon nanotube composites fabricated by microwave selective sintering. J Mater Chem C 2019;7(26):7938–46.
[19] Yang X, Fan S, Li Y, Guo Y, Li Y, Ruan K, Zhang S, Zhang J, Kong J, Gu J. Synchronously improved electromagnetic interference shielding and thermal conductivity for epoxy nanocomposites by constructing 3D copper nanowires/thermally annealed graphene aerogel framework. Compos A Appl 2020;128:105670.
[20] Krishnakumar B, Prasanna Sanka R, Binder W, Park C, Jung J, Parthasarthy V, Ran S, Yun G. Catalyst free self-healable vitrimer/graphene oxide nanocomposites. Compos B Eng 2020;184:107647.
[21] Al-Saleh MH. Electrical and electromagnetic interference shielding characteristics of GNP/UHMWPE composites. J Phys D Appl Phys 2016;49(19):195302–8.
[22] Xu L, Zhang X, Cui C, Ren P, Yan D, Li Z. Enhanced mechanical performance of segregated carbon nanotube/poly(lactic acid) composite for efficient electromagnetic interference shielding. Ind Eng Chem Res 2019;58(11):4454–61.
[23] Wu H, Jia L, Yan D, Gao J, Zhang X, Ren P, Li Z. Simultaneously improved electromagnetic interference shielding and mechanical performance of segregated carbon nanotube/polypropylene composite via solid phase molding. Compos Sci Technol 2018;156:87–94.
[24] Yan D, Pang H, Li B, Vajtai R, Xu L, Ren P, Wang J, Li Z. Structured reduced graphene oxide/polymer composites for ultra-efficient electromagnetic interference shielding. Adv Funct Mater 2015;25(4):559–66.
[25] Wang M, Zhang K, Dai X, Li Y, Guo J, Liu H, Li G, Tan Y, Zeng J, Guo Z. Enhanced electrical conductivity and piezoresistive sensing in multi-wall carbon nanotubes/polydimethylsiloxane nanocomposites via the construction of a self-segregated structure. Nanoscale 2017;9(31):11017–26.
[26] Imbernon L, Oikonomou EK, Norvez S, Leibler L. Chemically crosslinked yet reprocessable epoxidized natural rubber via thermo-activated disulfide rearrangements. Polym Chem 2015;6(23):4271–8.
[27] Lu YX, Guan Z. Olefin metathesis for effective polymer healing via dynamic exchange of strong carbon-carbon double bonds. J Am Chem Soc 2012;134(34):14226–31.
[28] Song K, Ye W, Gao X, Fang H, Zhang Y, Zhang Q, Li X, Yang S, Wei H, Ding Y. Synergy between dynamic covalent boronic ester and boron–nitrogen coordination: strategy for self-healing polyurethane elastomers at room temperature with unprecedented mechanical properties. Mater Horiz 2021;8(1):216–23.
[29] Montarnal D, Capelot M, Tournilhac F, Leibler L. Silica-like malleable materials from permanent organic networks. Science 2011;334:965–8.
[30] Fang H, Ye W, Ding Y, Winter HH. Rheology of the critical transition state of an epoxy vitrimer. Macromolecules 2020;53(12):4855–62.
[31] Scheutz GM, Lessard JJ, Sims MB, Sumerlin BS. Adaptable crosslinks in polymeric materials: resolving the intersection of thermoplastics and thermosets. J Am Chem Soc 2019;141(41):16181–96.
[32] Podgorski M, Fairbanks BD, Kirkpatrick BE, McBride M, Martinez A, Dobson A, Bongiardina NJ, Bowman CN. Toward stimuli-responsive dynamic thermosets

through continuous development and improvements in covalent adaptable networks (CANs). Adv Mater 2020;32(20):1906876.
[33] Shi Q, Yu K, Dunn ML, Wang T, Qi HJ. Solvent assisted pressure-free surface welding and reprocessing of malleable epoxy polymers. Macromolecules 2016;49(15):5527–37.
[34] Yu K, Shi Q, Li H, Jabour J, Yang H, Dunn ML, Wang T, Qi HJ. Interfacial welding of dynamic covalent network polymers. J Mech Phys Solid 2016;94:1–17.
[35] Yu K, Shi Q, Dunn ML, Wang TJ, Qi HJ. Carbon fiber reinforced thermoset composite with near 100% recyclability. Adv Funct Mater 2016;26(33):6098–106.
[36] Yang Y, Pei Z, Li Z, Wei Y, Ji Y. Making and remaking dynamic 3D structures by shining light on flat liquid crystalline vitrimer films without a mold. J Am Chem Soc 2016;138(7):2118–21.
[37] Yuan D, Guo H, Ke K, Manas ZI. Recyclable conductive epoxy composites with segregated filler network structure for EMI shielding and strain sensing. Compos A Appl 2020;132:105837–46.
[38] Capelot M, Unterlass MM, Tournilhac F, Leibler L. Catalytic control of the vitrimer glass transition. ACS Macro Lett 2012;1(7):789–92.
[39] Pu W, Fu D, Wang Z, Gan X, Lu X, Yang L, Xia H. Realizing crack diagnosing and self-healing by electricity with a dynamic crosslinked flexible polyurethane composite. Adv Sci 2018;5:1800101–10.
[40] Kuang X, Shi Q, Zhou Y, Zhao Z, Wang T, Qi HJ. Dissolution of epoxy thermosets via mild alcoholysis: the mechanism and kinetics study. RSC Adv 2018;8(3):1493–502.
[41] Han J, Liu T, Hao C, Zhang S, Guo B, Zhang J. A catalyst-free epoxy vitrimer system based on multifunctional hyperbranched polymer. Macromolecules 2018;51(17):6789–99.
[42] Yang X, Guo Y, Luo X, Zheng N, Ma T, Tan J, Li C, Zhang Q, Gu J. Self-healing, recoverable epoxy elastomers and their composites with desirable thermal conductivities by incorporating BN fillers via in-situ polymerization. Compos Sci Technol 2018;164:59–64.
[43] Wang M, Sheng J, Zhou S, Yang Z, Zhang X. Effect of free surface layer and interfacial zone on glass-transition behavior of PMMA/CNT nanocomposite. Macromolecules 2019;52(5):2173–80.
[44] Legrand A, Corinne SZ. Silica–epoxy vitrimer nanocomposites. Macromolecules 2016;49(16):5893–902.
[45] Tang Z, Huang Q, Liu Y, Chen Y, Guo B, Zhang L. Uniaxial stretching-induced alignment of carbon nanotubes in cross-linked elastomer enabled by dynamic cross-link reshuffling. ACS Macro Lett 2019;8(12):1575–81.
[46] Deng H, Lin L, Ji M, Zhang S, Yang M, Fu Q. Progress on the morphological control of conductive network in conductive polymer composites and the use as electroactive multifunctional materials. Prog Polym Sci 2014;39(4):627–55.
[47] Jia L, Yan D, Cui C, Jiang X, Ji X, Li Z. Electrically conductive and electromagnetic interference shielding of polyethylene composites with devisable carbon nanotube networks. J Mater Chem C 2015;3(36):9369–78.
[48] Wang L, Qiu H, Liang C, Song P, Han Y, Han Y, Gu J, Kong J, Pan D, Guo Z. Electromagnetic interference shielding MWCNT-Fe3O4@Ag/epoxy nanocomposites with satisfactory thermal conductivity and high thermal stability. Carbon 2019;141:506–14.
[49] Li J, Zhang G, Zhang H, Fan X, Zhou L, Shang Z, Shi X. Electrical conductivity and electromagnetic interference shielding of epoxy nanocomposite foams containing functionalized multi-wall carbon nanotubes. Appl Surf Sci 2018;428:7–16.
[50] Yue L, Pircheraghi G, Monemian SA, Manas ZI. Epoxy composites with carbon nanotubes and graphene nanoplatelets – dispersion and synergy effects. Carbon 2014;78:268–78.
[51] Clerc JP, Giraud G, Laugier JM, Luck JM. The electrical conductivity of binary disordered systems, percolation clusters, fractals and related models. Adv Phys 1990;39(3):191–309.
[52] Shen B, Zhai W, Tao M, Ling J, Zheng W. Lightweight, multifunctional polyetherimide/graphene@Fe_3O_4 composite foams for shielding of electromagnetic pollution. ACS Appl Mater Interfaces 2013;5(21):11383–91.
[53] Wang G, Wang L, Mark LH, Shaayegan V, Wang G, Li H, Zhao G, Park CB. Ultralow-threshold and lightweight biodegradable porous PLA/MWCNT with segregated conductive networks for high-performance thermal insulation and electromagnetic interference shielding applications. ACS Appl Mater Interfaces 2018;10(1):1195–203.
[54] Kuzhir P, Paddubskaya A, Bychanok D, Liubimau A, Ortona A, Fierro V, Celzard A. 3D-printed, carbon-based, lossy photonic crystals: is high electrical conductivity the must? Carbon 2021;171:484–92.